Geochemical Perspectives Letters

© 2021 The Authors
Published by the European Association of Geochemistry

Chlorine isotope ratios record magmatic brine assimilation during rhyolite genesis

E. Ranta, S.A. Halldórsson, J.D. Barnes, K. Jónasson, A. Stefánsson

Supplementary Information

The Supplementary Information includes:

- S-1: Samples and Methods
- S-2: Geological Setting
- S-3: Chlorine Contents in Icelandic Melt Inclusions
- S-4: Bulk Assimilation Model
- S-5: Quantifying Magmatic Brine Formation in the Crust
- Tables S-1 to S-3
- Figures S-1 to S-5
- Supplementary Information References

S-1: Samples and Methods

A total of 16 volcanic rocks from Iceland were analysed in this study (Tables S-1, S-2). New δ^{37}Cl data are reported for 14 of these samples (Table S-2). Together with the samples analysed by Halldórsson *et al.* (2016), they cover the main neovolcanic zones of Iceland, *i.e.*, the rift, propagating rift and rift zones, as well as the full geochemical range within these zones, *i.e.*, tholeiitic, transitional and alkaline magma suites (Fig. S-1, S-2). The basaltic (n = 3) and intermediate (n = 4) rocks are subglacial (HNAUS-1) or subaerial lavas. The silicic samples from this study (n = 8) and Halldórsson et al. (2016) (n = 3) are tephras (n = 5) and obsidians (n = 6). All material extracted from the samples for chemical analysis was chosen to be as fresh as possible and free from visible alteration. Therefore, any secondary low-T chlorine isotopic fractionation induced by hydrothermal or surface alteration of the rocks is considered unlikely. For all samples,

except for HNAUS-1, ASD1L and ASD14L, major element data has been published previously; by Óskarsson *et al.* (1982) for samples A-THO, A-ALK, B-ALK, D28a (same as SNS-32), I-DAC, I-ICE and SAL-76; by Jónasson (2007) for KER-3 and H-6; by Sverrisdóttir (2007) for H3a, H4 and H5. The samples are Holocene (< 10 ka) in age except for A-THO, D28a, KER-3, H-6, SAL-74 and SAL-76 that are Upper Pleistocene (< 0.8 Ma).

Major element, Cl and S concentrations for the obsidian glasses A-THO, A-ALK, D28a, H-6 and KER-3 were analysed at the Institute of Earth Sciences (IES), University of Iceland using a JEOL JXA-8230 SuperProbe electron probe microanalyser (EPMA). Major elements for the subglacial glass HNAUS-1 were determined with an ARL-SEMQ EPMA at IES, University of Iceland, using a setup described in Halldórsson *et al.* (2008). For this sample, the chlorine concentrations were analysed by secondary ion mass spectroscopy (SIMS) at the Department of Terrestrial Magnetism, Carnegie Institution of Washington, using methods described in Hauri *et al.* (2002). Major element composition of samples ASD1L and ASD14L were analysed at IES by inductively coupled plasma optical emission spectrometry (ICP-OES) using methods described in Momme *et al.* (2003), and the Cl concentrations with X-Ray fluoresence spectrometry (XRF) with analytical details described in Sigvaldason and Óskarsson (1976). For the five obsidians (A-THO, A-ALK, H-6, KER-3, D28a), the H_2O and CO_2 concentrations were determined by Fourier transform infrared spectroscopy (FTIR) at IES on 50-380 um thick, doubly polished glass wafers. The H_2O and CO_2 concentrations were calculated with Beer-Lambert's law

$$C = \frac{100MA}{\rho h \varepsilon} \qquad \text{Eq. S-1}$$

where M is the molar weight of the species [g/mol], A is the absorbance, ρ is density [g/L], h is the thickness of the glass wafer [cm] and ε is the absorptivity coefficient [L $mol^{-1}cm^{-1}$]. For the H_2O peak at 3500 cm^{-1}, a value of ε = 93.1 L $mol^{-1}cm^{-1}$ was used, determined experimentally for an Icelandic tholeiitic series rhyolite sample (KRA-045-2; McIntosh *et al.*, 2017). The CO_2 concentrations were below detection limit (c. 10 ppm) for all samples.

Chlorine and oxygen isotope ratios were measured at the University of Texas at Austin using methods described in the supplement of Halldórsson *et al.* (2016). For chlorine isotope analysis, 200-600 mg of sample powder was washed five times in 18 MΩ deionised water. Chloride ions were released by pyrohydrolysis, trapped in an aqueous solution and converted to AgCl. The AgCl was reacted with CH_3I to produce CH_3Cl. The CH_3Cl was purified on-line in a series of cryogenic traps and a gas chromatograph before introduction into a ThermoElectron MAT 253 isotope ratio mass spectrometer (IRMS). The reported error of 1σ = 0.2 ‰ is based on a long-term average of internal standards.

Oxygen isotope ratios for samples D28a, H-6, HNAUS-1, KER-3, and SAL-76 were determined on chips of ≈ 2 mg of sample by laser fluorination-IRMS using a CO_2 laser in a BF_5 atmosphere. The extracted O_2 was purified in a series of cryogenic traps before introduction into a ThermoElectron MAT 253 IRMS. Full methodology is described by Sharp (1990). An error of 1σ = 0.07 ‰ is based on the long-term reproducibility of $\delta^{18}O$ values of the San Carlos olivine ($\delta^{18}O$ = 5.25 ‰), Lausanne-1 quartz ($\delta^{18}O$ = 18.1 ‰) and UWG-2 garnet ($\delta^{18}O$ = 5.8 ‰) (Valley *et al.*, 1995) standards.

Oxygen isotope ratios for ASD1L, ASD14L, H3a, H4 and H5 were analysed from whole rock samples by Geochron Laboratories, Inc., Cambridge, Mass., in 1996 with conventional methods and have an analytical uncertainty of 1σ = 0.2 ‰.

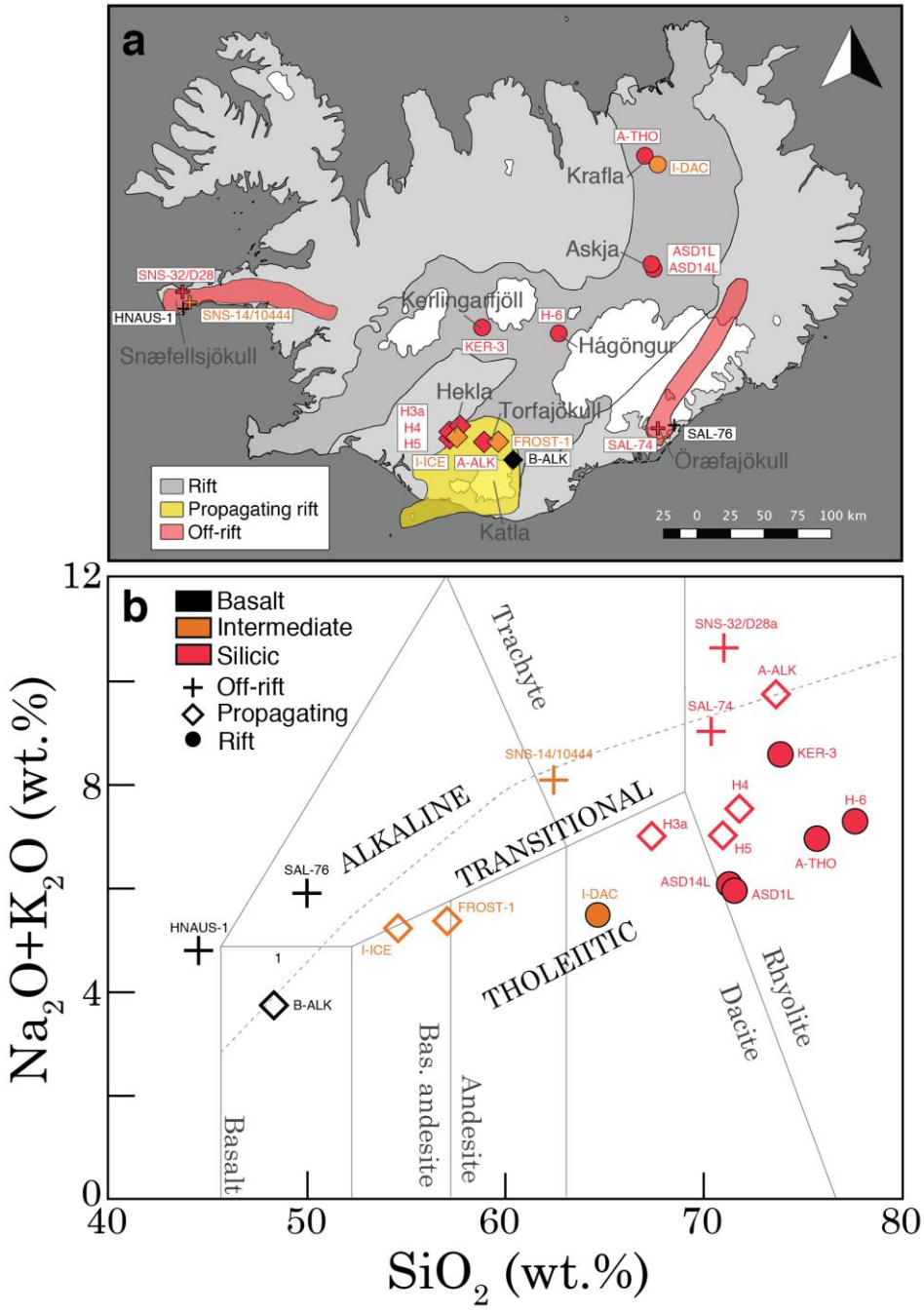

Figure S-1 **(a)** Sample map and classification. The neovolcanic zones in Iceland are indicated by grey field. Locations of samples used in this study are indicated by black (basalts), orange (intermediate) and red (silicic) circles (rift), diamonds (propagating rift) and crosses (off-rift). **(b)** Total alkali vs. SiO_2 diagram showing the geochemical range of the samples. The samples cover the Icelandic alkaline, transitional and tholeiitic magmatic suites.

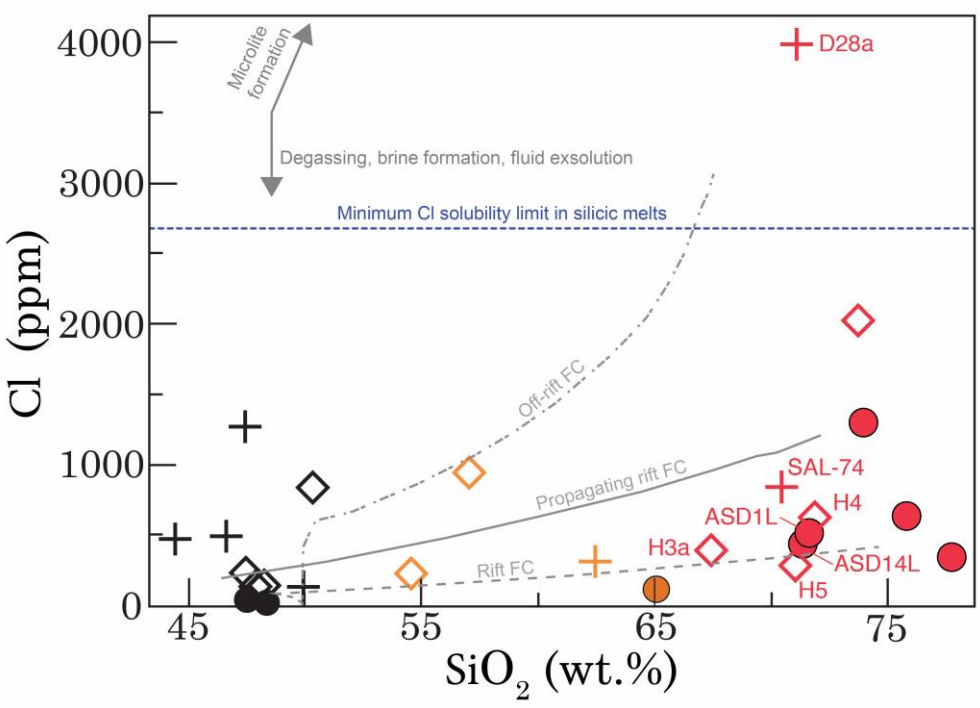

Figure S-2 Chlorine concentrations show an overall increase from low to high concentrations with increasing SiO_2 contents, compatible with isobaric fractional crystallisation models (using MELTS, c.f. Fig. S-3) for the different volcano-tectonic settings. Propagating rift and off-rift samples have generally higher Cl concentrations than the rift samples. However, the large spread in chlorine concentrations at a given SiO_2 content even within similar settings probably indicates the combined effect of different source concentrations, chlorine loss by degassing and fluid exsolution, increase during microlite formation upon cooling, and chlorine addition by assimilation of magmatic brines. Notably, all except one sample (D28a) plot below the estimated minimum Cl solubility limit in silicic melts (Metrich and Rutherford, 1992; Webster, 1997). Symbols as in Figure S-1.

S-2: Geological Setting

Rhyolites are rare in most oceanic islands but constitute up to 10 % of the crust of Iceland (Jónasson, 2007). Genesis of rhyolites in Iceland is favored by prolonged melt evolution in long-lived magmatic reservoirs beneath central volcanoes that sit on top of an unusually thick, up to 40 km, oceanic-type crust, which in turn is the result of excessive melt generation beneath Iceland. Icelandic rhyolite genesis is often seen as a modern analogue for how the first silicic continental crust on the planet may have emerged before the onset of plate tectonics (Willbold *et al.*, 2009; Reimink *et al.*, 2014).

Prevailing ideas suggest that silicic melts in Iceland have been created by (1) partial melting of hydrated basaltic crust, (2) fractional crystallisation of mantle-derived basaltic melts or (3) a combination of (1) and (2) (Nicholson *et al.*, 1991; Sigmarsson *et al.*, 1992; Gunnarsson *et al.*, 1998; Martin and Sigmarsson, 2010; Schattel *et al.*, 2014). Moreover, (1) and (2) are generally thought to dominate at two end-member volcano-tectonic settings: partial melting is favored at rift

zones where the geothermal gradient is high (*e.g.*, Askja, Krafla) (Martin and Sigmarsson, 2007; Kuritani *et al.*, 2011; Schattel *et al.*, 2014), whereas fractional crystallisation from basaltic parental melts seems to the dominant rhyolite forming process at the off-rift volcanoes (Snæfellsjökull, Öræfajökull) that are situated on top of colder crust (Prestvik *et al.*, 2001; Martin and Sigmarsson, 2010). An intermediate setting is represented by the non-rifting South Iceland Volcanic Zone (*e.g.*, Hekla, Torfajökull), which is the southward-propagating tip of the Eastern Rift Zone and is marked by high magma production rates and high frequency of rhyolitic eruptions, whose genesis is likely a combination of (1) and (2) (Gunnarsson *et al.*, 1998; Martin and Sigmarsson, 2010; Chekol *et al.*, 2011).

Possible correlation between volcano-tectonic setting and δ^{37}Cl – implications for magmatic brine formation

The negative δ^{37}Cl shifts in silicic rocks observed in this study seem to be larger at propagating rift and rift settings, but smaller or absent at off-rift settings (Figs. 1b and 2). This apparent correlation may be explained by considering how the volcano-tectonic setting is likely to influence how magmatic brine formation and assimilation take place. Silicic magma genesis below rift and propagating rift central volcanoes in Iceland takes place in hot (Martin and Sigmarsson, 2010; Schattel *et al.*, 2014) and dynamic mush systems that are maintained by frequent injections of fresh basaltic magma from underlying mafic domain or impinging rift dikes, which stimulate partial melting of wall rock and remobilisation of previously formed silicic segregations (Gunnarsson *et al.*, 1998; Jónasson 2007; Gurenko *et al.*, 2015). Such conditions promote magmatic brine formation. The off-rift systems reside in a colder crust, experience longer intervals without activity and are characterised by silicic magma generation that more closely resembles closed-system fractional crystallisation (Martin and Sigmarsson, 2010; Schattel *et al.*, 2014). In such environment, mushes are likely to be less developed, melts interact less with their surroundings, and the conditions for magmatic brine assimilation are suboptimal.

S-3: Chlorine Contents in Icelandic Melt Inclusions

Glassy melt inclusions (MI) potentially record the pre-eruptive volatile contents of the melts from which they crystallised and may hold information about the de- and regassing history of Cl within the crustal magma storage domain (Webster *et al.*, 2019). We compiled volatile concentration data in melt inclusions (MIs) in olivine, clinopyroxene and plagioclase in Icelandic basalts and rhyolites published before July 2020 with the aim of assessing degassing relationships between H_2O and Cl (Fig. S-3; Table S-3). Where available, the database includes data for paired matrix glass (MG) or whole-rock analyses, as well as MI major and trace element data. Values corrected for post-entrapment crystallisation are plotted as published.

MI and matrix glass Cl concentrations in Icelandic silicic rocks are similar (Fig. S-3a), suggesting that insignificant amount of syn-eruptive Cl degassing takes place, presumably caused by the slow diffusion of Cl compared to H_2O from melt into vapor bubbles (Baker and Balcone-Boissard, 2009; Barnes *et al.*, 2014). Chlorine concentrations in the silicic MIs are generally lower than predicted by fractional crystallisation (Fig. S-3b), and the wide range of Cl concentrations in silicic MIs suggests that Cl is affected by other pre-eruptive processes. In the case of rift and propagating rift samples, low and variable Cl concentrations may be explained by their formation mechanism which involves partial melting of

altered crust with low Cl contents. Melt Cl concentrations can also increase through assimilation of Cl-rich material such as brines (Webster *et al.*, 2019) and decrease by exsolution of hydrosaline fluids or assimilation of Cl poor material. Exsolution of a Cl-rich brine is not indicated by the MI data, because the Cl concentrations are lower than the solubility limit of Cl at the pressure range of the model of Webster *et al.* (2015) (up to 7 kbar) and below the lower end of solubility limits of Cl in rhyolitic melts in general of 2200-2700 ppm at 1 bar (Metrich and Rutherford, 1992; Webster, 1997). Chlorine may also be lost by partitioning to an aqueous vapor phase (Shinohara, 2009). Essentially, the Cl/H_2O ratio of the melt controls whether a melt will exsolve a hydrosaline fluid or a Cl-bearing aqueous vapor upon reaching saturation (Webster, 2004) . About half of the silicic Icelandic MIs record Cl/H_2O ratios above 0.05, which is the approximate threshold for hydrosaline liquid exsolution in granitic melts (Webster, 2004).

In conclusion, the published MI and matrix glass volatile data available for Icelandic volcanic systems demonstrates that Cl concentrations in MIs are highly variable and indistinguishable from the matrix glasses (Fig. S-3a). Furthermore, Cl concentrations are also decoupled from the MI H_2O concentrations (Fig. S-3e), which in turn are essentially controlled by magma storage depths and degassing during eruptions (Schattel *et al.*, 2014). The pre- and syn-eruptive processes that affect Cl systematics of silicic rocks in Iceland and elsewhere, *e.g.*, at Mono Craters, USA (Barnes *et al.*, 2014) seem to be complex compared to H_2O and not fully understood at present (Webster *et al.*, 2019).

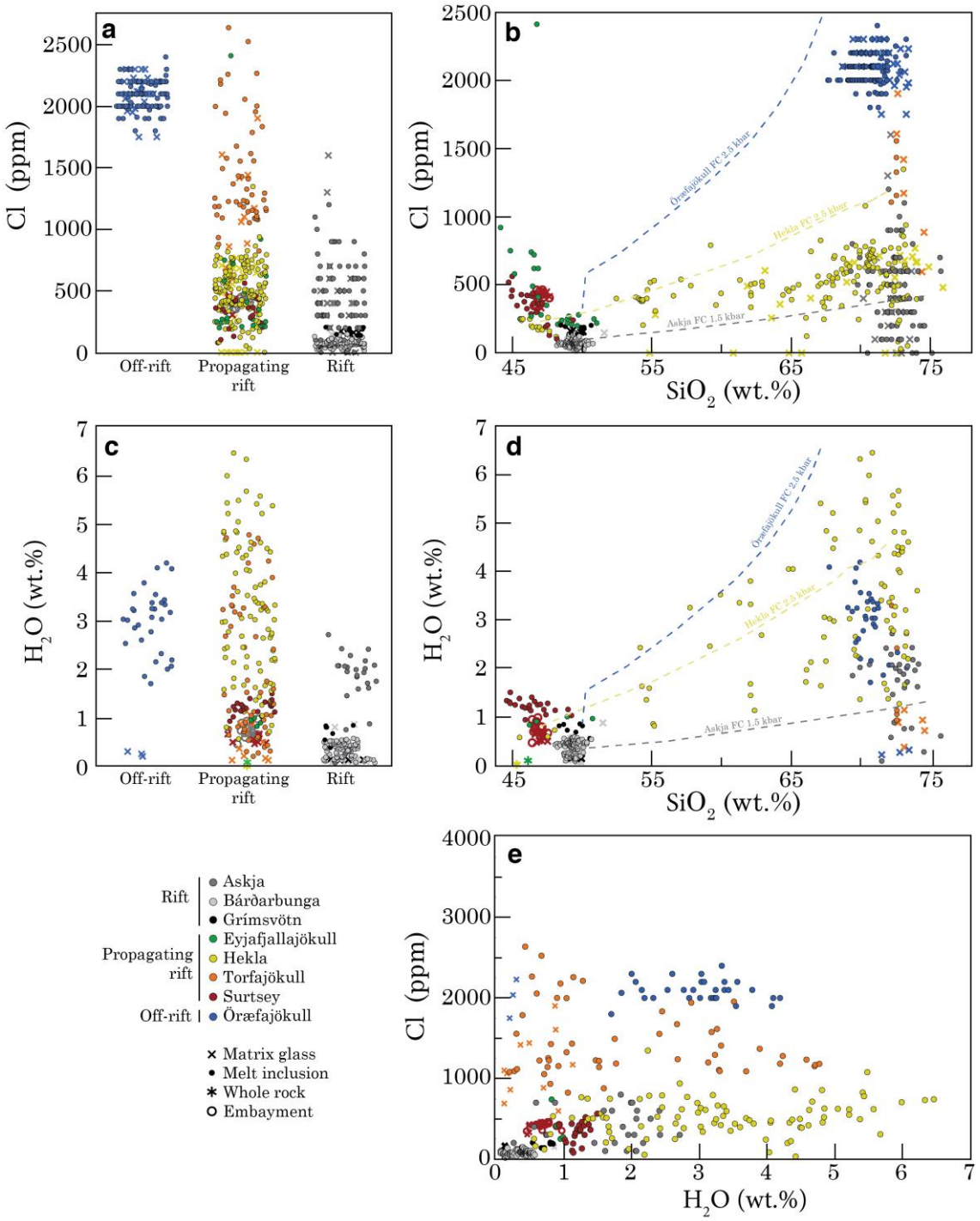

Figure S-3 **(a)-(e)** Compilation of published melt inclusion H_2O and Cl data from Iceland. The basaltic samples from different volcanic systems have variable Cl and H_2O concentrations depending on the degree of partial melting and, possibly, source volatile concentrations (Nichols *et al.*, 2002). This results in rift basalts with relatively low Cl and H_2O concentrations (Bárdarbunga, Grímsvötn) compared to alkaline basalts of Surtsey. Fractional crystallisation paths were calculated with the rhyolite-MELTS software (Gualda *et al.*, 2012; Ghiorso and Gualda, 2015). The total range in Cl conents of rhyolitic MIs from rift and propagating rift settings is large (< 50 to 2600 ppm) compared to Öræfajökull (1700-2400 ppm), the only rhyolitic off-rift volcano with available MI data. We take this difference to reflect the two different modes of rhyolite genesis in Iceland: at off-rift settings the pre-eruptive volatile history with respect to Cl is

seemingly simple and controlled by fractional crystallisation (Martin and Sigmarsson, 2010), while partial melting, assimilation as well as fluid exsolution and resorption processes at rift and propagating rift settings amount to a complex volatile history. The data was compiled from Moune *et al*. (2007), Sharma *et al*. (2008), Brounce *et al*. (2012), Moune *et al*. (2012), Portnyagin *et al*. (2012), Owen *et al*. (2013), Schattel et al. (2014), Lucic *et al*. (2016), Schipper *et al*. (2016) and Bali *et al*. (2018).

S-4: Bulk Assimilation Model

Bulk assimilation can be simulated with a binary mixing model (*e.g.*, Albarède, 1995). A binary mixture of a melt and an assimilant will attain the concentration C of element A of

$$C^A_{mix} = C^A_{assimilant} f_{assimilant} + C^A_{melt}(1-f_{assimilant}) \quad \text{Eq. S-2}$$

where $f_{assimilant}$ is the fraction of the assimilant. The mixture will have an isotopic ratio R of

$$R^A_{mix} = \rho^A_{melt} R^A_{melt} + \rho^A_{assimilant} R^A_{assimilant} \quad \text{Eq. S-3}$$

where the mixing parameters ρ^A_{melt} and $\rho^A_{assimilant}$ are defined as

$$\rho^A_{melt} = \frac{C^A_{melt}(1-f_{assimilant})}{C^A_{assimilant} f_{assimilant} + C^A_{melt}(1-f_{assimilant})} \quad \text{Eq. S-4}$$

$$\rho^A_{assimilant} = \frac{C^A_{assimilant} f_{assimilant}}{C^A_{melt}(1-f_{assimilant}) + C^A_{assimilant} f_{assimilant}} \quad \text{Eq. S-5}$$

For chlorine and oxygen, the isotopic ratios are converted to standard delta notation as

$$\delta^A = \frac{R^A_{mix} - R^A_{standard}}{R^A_{standard}} \times 1000\ ‰ \quad \text{Eq. S-6}$$

The isotopic ratios used for the international standards for chlorine (SMOC = Standard Mean Ocean Chloride) and oxygen (VSMOW = Vienna Standard Mean Ocean Water) were

$$R^{Cl}_{SMOC} = (^{37}Cl/^{35}Cl)_{SMOC} = 0.3188962681$$

$$R^{O}_{VSMOW} = (^{18}O/^{16}O)_{VSMOW} = 0.002005171$$

We performed assimilation modeling using the following hypothetical end-member compositions:

(1) Pristine rhyolite melt: Cl = 200 ppm, O = 48 wt.%, $\delta^{37}Cl$ = 0 ‰, $\delta^{18}O$ = 6.0 ‰ (the low Cl concentrations and the basalt-like $\delta^{18}O$ values are typical for Hekla rhyolites; Table S-2).

(2) Saline pore water (*e.g.*, mix of magmatic brine and meteoric-derived hydrothermal water): Cl = 20,000 ppm (NaCl equivalent = 3.3 wt.%), O = 83.1 wt.%, $\delta^{18}O$ = -10 ‰, $\delta^{37}Cl$ = -4.0 ‰ (the low $\delta^{18}O$ value representing high-latitude precipitation (Árnason, 1976)).

(3) Magmatic brine: Cl = 100,000 ppm ($NaCl_{equivalent}$ = 16.5 wt.%), O = 62.2 wt.%, $\delta^{18}O$ = 6.0 ‰, $\delta^{37}Cl$ = -4.0 ‰ (the $\delta^{18}O$ is assumed to be similar to pristine rhyolite melt).

(4) Hydrothermally altered crust: Cl = 500 ppm, O = 48 wt.%, $\delta^{18}O$ = -10.0 ‰, $\delta^{37}Cl$ = -4.0 ‰ (the Cl concentration is at the upper end of altered oceanic crust (Barnes and Cisneros, 2012) and the $\delta^{18}O$ value is at the lower end of altered crust in Iceland (Gautason and Muehlenbachs, 1998)).

Our choice of $\delta^{37}Cl$ = -4 ‰ for magmatic brine and saline pore fluid is less negative than the possible $\delta^{37}Cl$ = -5 ‰ demonstrated by Fortin *et al.* (2017). The model demonstrates that assimilation of hydrothermally altered basalt, even if ascribed a relatively high Cl concentration (500 ppm; Barnes and Cisneros, 2012) and an unrealistically low $\delta^{37}Cl$ value of -4 ‰ (see main text), is unable to explain the observed data (Fig. S-4) because unrealistically high degrees of assimilation (> 40 wt.%) would be required to explain the observed negative $\Delta^{37}Cl_{rhyolite\text{-}basalt}$ shifts.

Other globally known materials with distinctly negative $\delta^{37}Cl$ values include marine sediments (-3.0 to +0.7 ‰; Barnes and Sharp, 2017) and marine pore fluids (-7.8 to +0.3 ‰; Ransom *et al.*, 1995; Bonifacie *et al.*, 2007), but are not widespread in the Icelandic crust, which has not significantly interacted with seawater (Halldórsson *et al.*, 2016). Potential assimilation of clays with negative $\delta^{37}Cl$ values cannot readily explain the negative $\Delta^{37}Cl_{rhyolite\text{-}basalt}$ shifts as their Cl concentrations are generally similar to rhyolites (< 2000 ppm; Barnes *et al.*, 2008). Negative $\delta^{37}Cl$ values found in arc basalts (Barnes and Straub, 2010; Chiaradia *et al.*, 2014; Manzini *et al.*, 2017; Bouvier *et al.*, 2019) and some recycled mantle components (John *et al.*, 2010) are most likely related to Cl sourced from subducted slabs. While incorporation of recycled sediments in the Icelandic mantle has been suggested to explain the $\delta^{37}Cl$ variability of Icelandic basalts (Halldórsson *et al.*, 2016), it can not explain the negative $\delta^{37}Cl$ values of silicic rocks relative to the basalts.

Instead, all negative $\delta^{37}Cl$ values in this study can be explained by up to 0.5 wt.% assimilation of a magmatic brine (Fig. S-4). Notably, the $\delta^{18}O_{rhyolite}$ values resulting from fluid assimilation are relatively unsensitive to the $\delta^{18}O$ value of the assimilant, because only low degrees of assimilation are required, and because the oxygen concentrations of melts and fluids are of the same order (Fig. S-4b). For example, 2.5 wt.% assimilation of the saline pore fluid end member required for the maximum $\delta^{37}Cl$ shift of -2.9 ‰ leads only to a minor (-0.7 ‰) shift of the $\delta^{18}O$ value of the silicic melts despite a very low hypothetical $\delta^{18}O$ = -10 ‰ (Fig S-4b).

Lowered K/Cl ratios have been used to trace brine assimilation in mid-ocean ridge basalts (e.g. Kendrick et al. 2013, 2017) as K/Cl ratios are low in saline fluids and brines (<< 1) compared to the pristine basaltic melts (c. 10-100), and because the K/Cl ratio is not fractionated during fractional crystallisation of basalts. Compared to basaltic MIs (K/Cl ≈ 5-50), silicic MIs in Iceland show a considerably larger variation of K/Cl ratios at the propagating rift volcano Hekla (13-755) and the rift volcano Askja (16-291). This large variation is caused by the complicated controls on Cl concentrations in silicic melts (see section S-3). Because of the large variability in K/Cl ratios in silicic melts, assimilation of small amounts (< 1 wt.%) of magmatic brine is difficult to demonstrate using K/Cl (Fig. S-5). Figure S-5 demonstrates that δ^{37}Cl is a much more sensitive tracer of magmatic brine assimilation in silicic rocks than K/Cl.

Furthermore, we consider a fluid assimilant the most likely candidate for controlling the δ^{37}Cl signatures of silicic rocks because isotopes of non-volatile elements show that (1) rhyolites in Iceland generally preserve the long-lived radiogenic isotopic (Sr-Nd-Hf-Pb) signatures of corresponding basalts confirming that the source material of the refractory elements is ultimately basalt from the same system (Sigmarsson *et al.*, 1992 ; Kuritani *et al.*, 2011), and (2) extensive previous work on multiple non-volatile stable isotopes in Hekla samples, where the largest $\Delta^{37}Cl_{rhyolite\text{-}basalt}$ shifts are seen, conclude that the δ^{7}Li, δ^{41}K, δ^{66}Zn, δ^{98}Mo and ε^{205}Tl systematics show no difference between rhyolites and basalts from Hekla (Schuessler *et al.*, 2009; Chen *et al.*, 2013; Yang *et al.*, 2015; Prytulak *et al.*, 2017; Tuller-Ross, 2019), or that, in the case of δ^{30}Si, δ^{49}Ti, δ^{51}V, $\delta^{56/54}$Fe and $\delta^{94/90}$Zr, can be fully explained by fractional crystallisation (Schuessler *et al.*, 2009; Savage *et al.*, 2011; Prytulak *et al.*, 2016; Deng *et al.*, 2019; Inglis *et al.*, 2019).

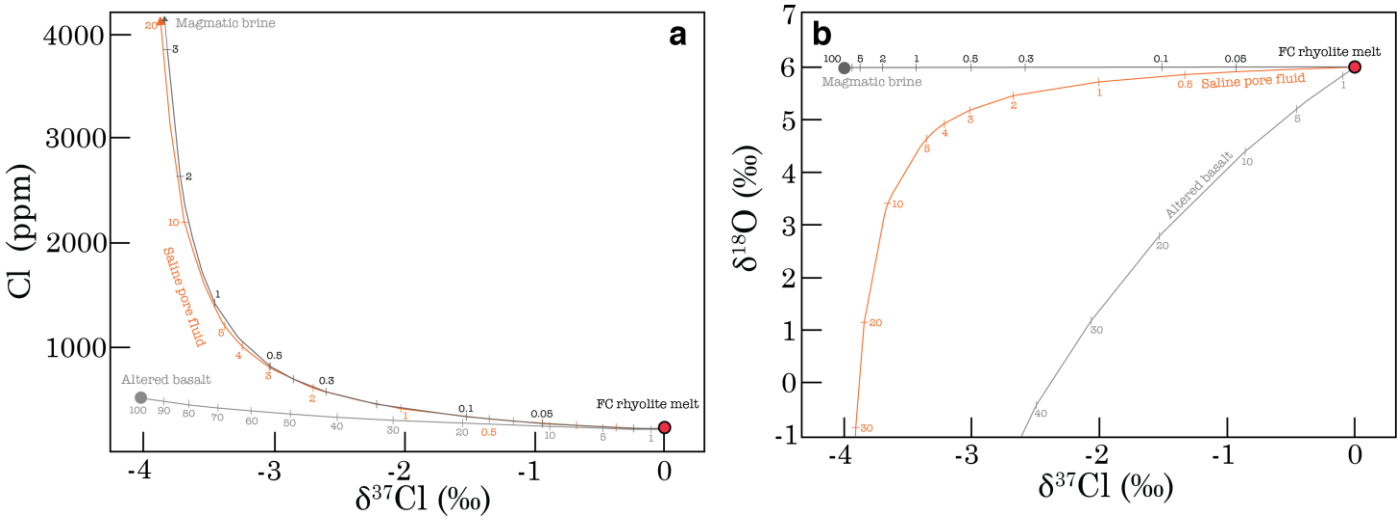

Figure S-4 **(a)-(b)** The effects of bulk assimilation of magmatic brine, saline pore fluid and hydrothermally altered crust on Cl, δ^{18}O and δ^{37}Cl values on pristine (unaffected by assimilation) rhyolite melt. See text for the used assimilant compositions.

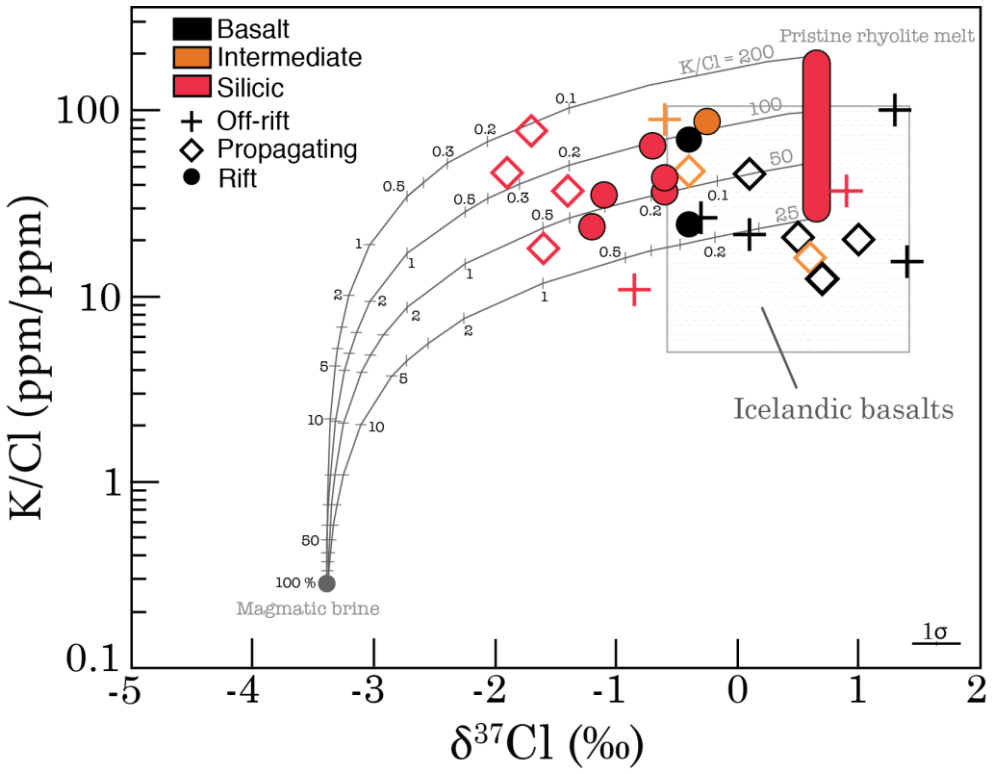

Figure S-5 The effect of bulk assimilation of magmatic brine on K/Cl and δ^{37}Cl values of rhyolitic melt. Small amount of magmatic brine assimilation does not generate K/Cl ratios subceeding the K/Cl range of basalts. Grey curves show binary mixing curves between magmatic brine with K/Cl = 0.28 (calculated for a brine with 10 wt.% Cl dissolved as $Na_{0.5}K_{0.5}Cl$, comparable to brine inclusions analysed by Audétat and Pettke (2003)) and pristine rhyolite melts with variable K/Cl ratios (25-200), K = 20,000 ppm. The δ^{37}Cl compositions of magmatic brine and pristine rhyolite melt are shifted by +0.7 ‰ compared to the end-member compositions defined in section S-4, so that the value of pristine rhyolite melts reflects the average δ^{37}Cl value of +0.7 ‰ of the propagating rift basalts. Note that binary mixing curves in K/Cl-δ^{37}Cl space are linear, but are here plotted on a logarithmic y-axis.

S-5: Quantifying Magmatic Brine Formation in the Crust

In the following, we assess (1) how much magmatic brine is expected to exsolve from magmatic intrusions, and (2) whether this production would be enough to sustain assimilation of 0.3 wt.% brine in extrusive silicic rocks, which is enough to explain most negative δ^{37}Cl shifts in rhyolites in this study (Fig. S-5).

Our estimate for brine assimilation, A = 0.3 wt.% (mass of assimilated brine/mass of erupted rhyolite), with salinity of Cl = 10 wt.% or NaCl = 16.5 wt.% (see previous section), corresponds to a volume ratio for brine/melt of about 0.006 (using densities of ρ_{melt} = 2260 kg/m^3 and ρ_{brine} = 1200 kg/m^3). For a hypothetical cylindrical silicic magma chamber with a thickness of 50 m, this corresponds to an overlaying brine layer with a thickness of c. 0.3 m, or equivalently, a 6 m thick mush layer with 5% porosity that is occupied by brine. This estimate can be compared to a > 1 km thick low-resistivity layer below the Merapi volcano, Indonesia, interpreted as saline fluids of possible magmatic origin residing

in host rock of 15% porosity (Müller and Haak, 2004). To convert A to a maximum brine assimilation rate B_a (kg of brine assimilated/yr) in Iceland, we use a silicic extrusion rate of R_e = 0.004 km^3/yr estimated for silicic historic eruptions (Thordarson and Larsen, 2007). Thus,

$$B_a = \rho_{melt} \times R_e \times A \approx 27 \times 10^6 \text{ kg/yr} \quad \text{Eq. S-7}$$

To estimate how much brine can be produced by magmatic intrusions, R_b (kg brine/yr) *i.e.*, magma that stalls and crystallises in the crust without erupting, we use

$$R_b = \rho_{melt} \times R_i \times F \quad \text{Eq. S-8}$$

where F is the mass ratio of exsolved brine/intrusive melt and R_i is derived from the magmatic intrusion/extrusion production ratio X,

$$X = R_i/R_e \quad \text{Eq. S-9}$$

We choose a value of X = 5, which is considered plausible for Iceland (White *et al.*, 2006), yielding a silicic intrusion rate for Iceland of R_i = 0.02 km^3/yr. The most difficult parameter to estimate in Eq. S-8 is F. An effort to estimate fluid/melt ratios and the salinities of exsolved fluids from a global compilation of silicic MIs was recently undertaken by Webster *et al.* (2019). The Cl contents of fluids exsolved from magmas range from 0.3 to up towards 70 wt. % for low fluid/melt ratios of F = 2 x 10^{-3} (by mass) and 0.3-11 wt.% for a higher fluid/melt estimate of F = 4.7 x 10^{-2}, *i.e.*, lower fluid/melt ratios generate higher salinity fluids (Webster *et al.*, 2019). A brine can alternatively be created from a supersolvus fluid with moderate NaCl concentrations by unmixing to a low-NaCl vapor and a high-NaCl liquid upon hitting a solvus curve at 1.3-1.5 kbar (Webster and Mandeville, 2007; Audétat *et al.*, 2008), or alternatively, by vapor condensation (Audétat *et al.*, 2008; Giggenbach *et al.*, 2003). For example, a supersolvus fluid exsolved from a melt with a relatively high fluid/melt ratio of 2 x 10^{-2} but a relatively low salinity of NaCl = 2 wt.% would unmix upon decompression from 1.5 kbar to 1 kbar to form vapor with about NaCl = 1 wt.% and a liquid with NaCl = 11 wt.% with vapor/liquid mass proportions of 10. In this case, the effective brine/melt ratio with respect to original melt would be 2 x 10^{-3}. In the following calculations we use a range of brine/melt ratios of F = 2 x 10^{-3} to 5 x 10^{-3}, which we consider to be a realistic estimate for generating a brine with an average $NaCl_{equivalent}$ = 16.5 wt.% from crystallising intrusions (the concentration used in our assimilation model).

Using these estimates, Eq. S-8 yields magmatic brine production rates of 90-226 x 10^6 kg/yr from silicic intrusions in Iceland. Thus, the supply of brines from crystallizing intrusions is likely to exceed the amount of brine assimilation required to explain the observed δ^{37}Cl signatures in Icelandic rhyolites by a factor of 3 to 8.

Supplementary Tables

Table S-1 Sample information.

Sample	Volcanic system	Location/eruption	Rock type	Class	Setting	Type
ASD1L	Askja	1875 eruption	Rhyolite	Silicic	Rift	Tephra
ASD14L	Askja	1875 eruption	Rhyolite	Silicic	Rift	Tephra
A-THO[a]	Krafla	Hrafntinnuhryggur	Rhyolite	Silicic	Rift	Obsidian
I-DAC	Krafla	Hraunbunga	Dacite	Intermediate	Rift	Lava
KER-3	Kerlingarfjöll	Ögmundur	Rhyolite	Silicic	Rift	Obsidian
H-6	Hágöngur	Hágöngur	Rhyolite	Silicic	Rift	Obsidian
SNS-32/D28a	Snæfellsjökull	Mælifell	Rhyolite	Silicic	Off-rift	Obsidian
SNS-14/10444	Snæfellsjökull	Háahraun	Dacite	Intermediate	Off-rift	Lava
HNAUS-1	Snæfellsjökull	Hnausagil	Basanite	Basalt	Off-rift	Subglacial
SAL-74[a]	Öræfajökull	Kvísker	Rhyolite	Silicic	Off-rift	Obsidian
SAL-76	Öræfajökull	Kálfafellsdalur	Trachybasalt	Basalt	Off-rift	Lava
A-ALK[a]	Torfajökull	Hrafntinnusker	Alkali rhyolite	Silicic	Propag. rift	Obsidian
H3a	Hekla	H3	Dacite	Silicic	Propag. rift	Tephra
H4	Hekla	H4	Rhyolite	Silicic	Propag. rift	Tephra
H5	Hekla	H5	Rhyolite	Silicic	Propag. rift	Tephra
I-ICE	Hekla	Hekla 1970	Icelandite	Intermediate	Propag. rift	Lava
B-ALK	Katla	Eldgjá	Fe-Ti Basalt	Basalt	Propag. rift	Lava

[a]Halldórsson *et al.* (2016)

Table S-2 Sample data.

Sample	$\delta^{37}Cl$ ‰	$\delta^{18}O$ ‰	SiO_2 wt.%	TiO_2 wt.%	Al_2O_3 wt.%	FeO_{tot} wt.%	MnO wt.%	MgO wt.%	CaO wt.%	Na_2O wt.%	K_2O wt.%	P_2O_5 wt.%	Total wt.%	n (EPMA)	H_2O wt.%	± 1σ (n=6)	CO_2 ppm
ASD1L[b]	-0.6	-0.50	71.62	0.85	12.83	4.32	0.11	0.99	2.96	3.70	2.26	0.20			0.51		
ASD14L[b]	-0.9	0.70	71.35	0.87	12.85	4.30	0.10	0.91	3.11	3.80	2.28	0.25			0.14		
duplicate	-0.3																
A-THO[a]	-1.1	2.82	75.80	0.23	12.19	3.20	0.09	0.09	1.68	4.28	2.68	0.02	100.36	6	0.08	0.01	b.d.
I-DAC[c]	-0.1	4.20	64.68	0.88	15.26	6.02	0.12	1.46	4.83	4.12	1.37	0.21			0.45		
duplicate	-0.4																
KER-3	-1.2	4.40	73.95	0.18	13.13	2.54	0.07	0.06	0.92	4.89	3.71	0.02	99.60	6	0.13	0.004	b.d.
H-6	-0.7	4.74	77.74	0.15	11.57	2.17	0.05	0.00	0.92	4.64	2.66	0.02	99.96	6	0.10	0.02	b.d.
SNS-32/D28a	-0.6	5.37	71.09	0.16	14.06	2.58	0.14	0.05	0.45	5.45	5.21	0.01	99.60	6	0.08	0.02	b.d.
duplicate	-1.1	5.67															
SNS-14/10444[d]	-0.5	5.3	62.45	0.90	16.15	6.96	0.18	0.70	3.28	4.75	3.35	0.20			0.18		
duplicate	-0.7																
HNAUS-1	-0.3	5.05	44.43	4.23	12.22	14.07	0.30	5.20	10.47	3.30	1.50	0.84			0.12		10
SAL-74[a]	0.9	6.10	70.44	0.19	14.10	2.93	0.08	0.10	1.14	5.30	3.74	0.01			0.84		
SAL-76	1.2	4.35	49.93	2.56	16.36	11.45	0.22	4.15	7.00	4.33	1.58	0.84			0.48		
duplicate	1.4																
A-ALK[a]	-1.6	4.08	73.72	0.20	12.41	3.08	0.07	0.05	0.39	5.35	4.42	0.02	99.89	6	0.08	0.01	b.d.
H3a[b]	-1.9	5.76	67.42	0.39	14.57	5.07	0.16	0.30	2.95	4.84	2.17	0.07			1.28		
H4[b]	-1.4	5.70	71.86	0.18	13.02	2.33	0.09	0.07	1.55	4.77	2.78	0.00			2.53		
H5[b]	-1.7	5.57	71.03	0.47	13.97	4.14	0.12	0.42	2.57	4.38	2.64	0.12					
I-ICE[d]	-0.4	4.8	54.55	2.02	14.50	11.69	0.27	2.95	6.96	3.95	1.28	1.02			0.29		
B-ALK[d]	0.1	4.3	48.25	4.22	12.38	14.52	0.22	5.35	10.00	2.97	0.77	0.56			0.25		

Table S-2 (Continued)

Sample	F	Cl	S	Reference for major and volatile element concentrations
ASD1L[b]	466	513		this study
ASD14L[b]	382	435		this study
duplicate				
A-THO[a]		634	41	this study
I-DAC[a]	350	130		Óskarsson *et al.* (1982)
duplicate				
KER-3		1298	24	this study
H-6		342	26	this study
SNS-32/D28a		3988	28	this study
duplicate				
SNS-14/10444[d]	1260	310		Óskarsson *et al.* (1982)
duplicate				
HNAUS-1	1101	470	52	this study
SAL-74[a]	1080	840		Óskarsson *et al.* (1982)
SAL-76	752	130		Óskarsson *et al.* (1982)
duplicate				
A-ALK[a]		2024	23	this study
H3a[b]	1084	390		Sverrisdóttir (2007)
H4[b]	1424	624		Sverrisdóttir (2007)
H5[b]		282[e]		Sverrisdóttir (2007)
I-ICE[d]	1230	225		Óskarsson *et al.* (1982)
B-ALK[d]	443	140		Óskarsson *et al.* (1982)

[a]$\delta^{18}O$ and $\delta^{37}Cl$ data from Halldórsson *et al.* (2016) except for the $\delta^{18}O$ value of SAL-74, which is from Condomines *et al.* (1983)

[b]$\delta^{18}O$ values measured on whole rock by Geochron Laboratories, Inc., Cambridge, Mass.

[c]$\delta^{18}O$ value from Jónasson (2005)

[d]$\delta^{18}O$ value from Óskarsson *et al.* (1982)

[e]Cl concentration was determined based on the IRMS peak area and calibrated with internal standards of known Cl concentration.

Supplementary Data Table

A compilation of published melt inclusion H_2O and Cl data from Iceland (n = 725) is presented in Table S-3, which can be downloaded as a separate Excel file at http://www.geochemicalperspectivesletters.org/article2101. The data was compiled from Moune *et al*. (2007), Sharma *et al*. (2008), Brounce *et al*. (2012), Moune *et al*. (2012), Portnyagin *et al*. (2012), Owen *et al*. (2013), Schattel *et al*. (2014), Lucic *et al*. (2016), Schipper *et al.* (2016) and Bali *et al.* (2018).

Supplementary Information References

Albarède, F. (1995) *Introduction to geochemical modeling*. Cambridge University Press, New York.

Audétat, A., Pettke, T. (2003) The magmatic-hydrothermal evolution of two barren granites: A melt and fluid inclusion study of the Rito del Medio and Canada Pinabete plutons in northern New Mexico (USA). *Geochimica et Cosmochimica Acta* 67, 97–121.

Baker, D.R., Balcone-Boissard, H. (2009) Halogen diffusion in magmatic systems: Our current state of knowledge. *Chemical Geology* 263, 82–88.

Barnes, J.D., Straub, S.M. (2010) Chorine stable isotope variations in Izu Bonin tephra: implications for serpentinite subduction. *Chemical Geology* 272, 62–74.

Barnes, J.D., Cisneros, M. (2012) Mineralogical control on the chlorine isotope composition of altered oceanic crust. *Chemical Geology* 326, 51–60.

Bali, E., Hartley, M.E., Halldórsson, S.A., Gudfinnsson, G.H., Jakobsson, S. (2018) Melt inclusion constraints on volatile systematics and degassing history of the 2014–2015 Holuhraun eruption, Iceland. *Contributions to Mineralogy and Petrology* 173, 9.

Bouvier, A.S., Manzini, M., Rose-Koga, E.F., Nichols, A.R., Baumgartner, L.P. (2019) Tracing of Cl input into the sub-arc mantle through the combined analysis of B, O and Cl isotopes in melt inclusions. *Earth and Planetary Science Letters 507*, 30–39.

Brounce, M., Feineman, M., LaFemina, P., Gurenko, A. (2012) Insights into crustal assimilation by Icelandic basalts from boron isotopes in melt inclusions from the 1783–1784 Lakagígar eruption. *Geochimica et Cosmochimica Acta* 94, 164–180.

Chen, H., Savage, P.S., Teng, F.Z., Helz, R.T., Moynier, F. (2013) Zinc isotope fractionation during magmatic differentiation and the isotopic composition of the bulk Earth. *Earth and Planetary Science Letters* 369, 34–42.

Chekol, T.A., Kobayashi, K., Yokoyama, T., Sakaguchi, C., Nakamura, E. (2011) Timescales of magma differentiation from basalt to andesite beneath Hekla volcano, Iceland: constraints from U-series disequilibria in lavas from the last quarter-millennium flows. *Geochimica et Cosmochimica Acta* 75, 256–283.

Chiaradia, M., Barnes, J.D., Cadet-Voisin, S. (2014) Chlorine stable isotope variations across the Quaternary volcanic arc of Ecuador. *Earth and Planetary Science Letters* 396, 22–33.

Condomines, M., Grönvold, K., Hooker, P.J., Muehlenbachs, K., O'Nions, R.K., Oskarsson, N., Oxburgh, E.R. (1983) Helium, oxygen, strontium and neodymium isotopic relationships in Icelandic volcanics. *Earth and Planetary Science Letters* 66, 125–136.

Deng, Z. Chaussidon, M., Savage, P., Robert, F., Pik, R., Moynier, F. (2019) Titanium isotopes as a tracer for the plume or island arc affinity of felsic rocks. *Proceedings of the National Academy of Sciences USA* 116, 1132–1135.

Giggenbach, W.F., Shinohara, H., Kusakabe, M., Ohba, T. (2003) Formation of acid volcanic brines through interaction of magmatic gases, seawater, and rock within the White Island volcanic-hydrothermal system, New Zealand. *The Society of Economic Geologists Special Pubication* 10, 19-40.

Gualda, G.A., Ghiorso, M.S., Lemons, R.V., Carley, T.L. (2012) Rhyolite-MELTS: a modified calibration of MELTS optimized for silica-rich, fluid-bearing magmatic systems. *Journal of Petrology* 53, 875–890.

Gunnarsson, B., Marsh, B.D., Taylor Jr., H.P. (1998) Generation of Icelandic rhyolites: silicic lavas from the Torfajökull central volcano. *Journal of Volcanology and Geothermal Research* 83, 1–45.

Gurenko, A.A., Bindeman, I.N., Sigurdsson, I.A. (2015) To the origin of Icelandic rhyolites: insights from partially melted leucocratic xenoliths. *Contributions to Mineralogy and Petrology* 169, 49.

Ghiorso, M.S., Gualda, G.A. (2015) An H_2O–CO_2 mixed fluid saturation model compatible with rhyolite-MELTS. *Contributions to Mineralogy and Petrology* 169, 53.

Halldórsson, S.A., Óskarsson, N., Grönvold, K., Sigurdsson, G., Sverrisdóttir, G., Steinthórsson, S. (2008) Isotopic-heterogeneity of the Thjorsa lava—implications for mantle sources and crustal processes within the Eastern Rift Zone, Iceland. *Chemical Geology* 255, 305–316.

Hauri, E., Wang, J., Dixon, J.E., King, P.L., Mandeville, C., Newman, S. (2002) SIMS analysis of volatiles in silicate glasses: 1. Calibration, matrix effects and comparisons with FTIR. *Chemical Geology* 183, 99–114.

Inglis, E.C., Moynier, F., Creech, J., Deng, Z., Day, J.M.D., Teng, F.Z., Bizzarro, M., Jackson, M., Savage, P. (2019) Isotopic fractionation of zirconium during magmatic differentiation and the stable isotope composition of the silicate Earth. *Geochimica et Cosmochimica Acta* 250, 311–323.

Jónasson, K. (2005) Magmatic evolution of the Heiðarsporður ridge, NE-Iceland. *Journal of Volcanology and Geothermal Research* 147, 109–124.

Kendrick, M. A., Hémond, C., Kamenetsky, V. S., Danyushevsky, L., Devey, C. W., Rodemann, T., Jackson, M.G., Perfit, M. R. (2017) Seawater cycled throughout Earth's mantle in partially serpentinized lithosphere. *Nature Geoscience* 10, 222–228.

Kuritani, T., Yokoyama, T., Kitagawa, H., Kobayashi, K., Nakamura, E. (2011) Geochemical evolution of historical lavas from Askja Volcano, Iceland: implications for mechanisms and timescales of magmatic differentiation. *Geochimica et Cosmochimica Acta* 75, 570–587.

Lucic, G., Berg, A.S., Stix, J. (2016) Water-rich and volatile-undersaturated magmas at Hekla volcano, Iceland. *Geochemistry, Geophysics, Geosystems* 17, 3111–3130.

Manzini, M., Bouvier, A., Barnes, J.D., Bonifacie, M., Rose-Koga, E.F., Ulmer, P., Métrich, N., Bardoux, G., Williams, J., Layne, G.D., Straub, S., Baumgartner, L.P., John, T. (2017) SIMS chlorine isotope analyses in melt inclusions from arc settings. *Chemical Geology* 449, 112–122.

Martin, E., Sigmarsson, O. (2007) Crustal thermal state and origin of silicic magma in Iceland: the case of Torfajökull, Ljósufjöll and Snæfellsjökull volcanoes. *Contributions to Mineralogy and Petrology* 153, 593-605.

Martin, E., Sigmarsson, O. (2010) Thirteen million years of silicic magma production in Iceland: Links between petrogenesis and tectonic settings. *Lithos* 116, 129–144.

McIntosh, I.M., Nichols, A.R., Tani, K., Llewellin, E.W. (2017) Accounting for the species-dependence of the 3500 cm^{-1} $H2O_t$ infrared molar absorptivity coefficient: Implications for hydrated volcanic glasses. *American Mineralogist* 102, 1677-1689.

Metrich, N., Rutherford, M.J. (1992) Experimental study of chlorine behavior in hydrous silicic melts. *Geochimica et Cosmochimica Acta* 56, 607–616.

Momme, P., Óskarsson, N. & Keays, R.R. (2003) Platinum-group elements in the Icelandic rift system: melting processes and mantle sources beneath Iceland. *Chemical Geology* 196, 209–234.

Moune, S., Sigmarsson, O., Thordarson, T., Gauthier, P.J. (2007) Recent volatile evolution in the magmatic system of Hekla volcano, Iceland. *Earth and Planetary Science Letters* 255, 373–389.

Moune, S., Sigmarsson, O., Schiano, P., Thordarson, T., Keiding, J.K. (2012) Melt inclusion constraints on the magma source of Eyjafjallajökull 2010 flank eruption. *Journal of Geophysical Research* 117, B00C07.

Müller, A, Haak, V. (2004) 3-D modeling of the deep electrical conductivity of Merapi volcano (Central Java): integrating magnetotellurics, induction vectors and the effects of steep topography. *Journal of Volcanology and Geothermal Research* 138, 205–222.

Nichols, A.R. L., Carroll, M.R., Höskuldsson, A. (2002) Is the Iceland hot spot also wet? Evidence from the water contents of undegassed submarine and subglacial pillow basalts. *Earth and Planetary Science Letters* 202, 77–87.

Nicholson, H., Condomines, M., Fitton, J.G., Fallick, A.E., Grönvold, K., Rogers, G. (1991) Geochemical and isotopic evidence for crustal assimilation beneath Krafla, Iceland. *Journal of Petrology* 32, 1005–1020.

Óskarsson, N., Sigvaldason, G.E., Steinthorsson, S.A (1982) dynamic model of rift zone petrogenesis and the regional petrology of Iceland. *Journal of Petrology* 23, 28–74.

Owen, J., Tuffen, H., McGarvie, D.W. (2013) Explosive subglacial rhyolitic eruptions in Iceland are fuelled by high magmatic H_2O and closed-system degassing. *Geology* 41, 251–254.

Portnyagin, M., Hoernle, K., Storm., S., Mironov, N., van den Bogaard, C., Botcharnikov, R. (2012) H_2O-rich melt inclusions in fayalitic olivine from Hekla volcano: Implications for phase relationships in silicic systems and driving forces of explosive volcanism on Iceland. *Earth and Planetary Science Letters* 357, 337–346.

Prestvik, T., Goldberg, S., Karlsson, H., Grönvold, K. (2001) Anomalous strontium and lead isotope signatures in the off-rift Öræfajökull central volcano in south-east Iceland: evidence for enriched endmember (s) of the Iceland mantle plume? *Earth and Planetary Science Letters* 190, 211–220.

Prytulak, J., Sossi, P.A., Halliday, A.N., Plank, T., Savage, P.S., Woodhead, J.D. (2016) Stable vanadium isotopes as a redox proxy in magmatic systems? *Geochemical Perspectives Letters* 3, 75–84.

Prytulak, J., Brett, A., Webb, A., Plank, T., Rehkämper, M., Savage, P.S., Woodhead, J. (2017) Thallium elemental behavior and stable isotope fractionation during magmatic processes. *Chemical Geology* 448, 71–83.

Ransom, B., Spivack, A.J., Kastner, M. (1995) Stable Cl isotopes in subduction-zone pore waters: Implications for fluid-rock reactions and the cycling of chlorine. *Geology* 23**,** 715–718.

Reimink, J. R., Chacko, T., Stern, R.A., Heaman, L.M. (2014) Earth's earliest evolved crust generated in an Iceland-like setting. *Nature Geoscience* 7, 529.

Savage, P.S., Georg, R.B., Williams, H.M., Burton, K.W., Halliday, A.N. (2011) Silicon isotope fractionation during magmatic differentiation. *Geochimica et Cosmochimica Acta* 75, 6124–6139.

Schattel, N., Portnyagin, M., Golowin, R., Hoernle, K., Bindeman, I. (2014) Contrasting conditions of rift and off-rift silicic magma origin on Iceland. *Geophysical Research Letters* 41, 5813–5820.

Schipper, C.I., Le Voyer, M., Moussallam, Y., White, J.D.L., Thordarson, T., Kimura, J., Chang, Q. (2016) Degassing and magma mixing during the eruption of Surtsey Volcano (Iceland, 1963–1967): the signatures of a dynamic and discrete rift propagation event. *Bulletin of Volcanology* 78, 33.

Schuessler, J.A., Schoenberg, R., Sigmarsson, O. (2009) Iron and lithium isotope systematics of the Hekla volcano, Iceland—

evidence for Fe isotope fractionation during magma differentiation. *Chemical Geology* 258, 78–91.

Sharma, K., Self, S., Blake, S., Thordarson, T., Larsen, G. (2008) The AD 1362 Öræfajökull eruption, SE Iceland: Physical volcanology and volatile release. *Journal of Volcanology and Geothermal Research* 178, 719–739.

Sharp, Z.D. (1990) A laser-based microanalytical method for the in situ determination of oxygen isotope ratios of silicates and oxides. *Geochimica et Cosmochimica Acta* 54, 1353–1357.

Shinohara, H. (2009) A missing link between volcanic degassing and experimental studies on chloride partitioning. *Chemical Geology* 263, 51–59.

Sigmarsson, O., Condomines, M., Fourcade, S. (1992) A detailed Th, Sr and O isotope study of Hekla: differentiation processes in an Icelandic volcano. *Contributions to Mineralogy and Petrology* 112, 20–34.

Sigvaldason, G.E., Óskarsson, N. (1976) Chlorine in basalts from Iceland. *Geochimica et Cosmochimica Acta* 40, 777–789.

Sverrisdottir, G. (2007) Hybrid magma generation preceding Plinian silicic eruptions at Hekla, Iceland: evidence from mineralogy and chemistry of two zoned deposits. *Geological Magazine* 14, 643–659.

Thordarson, T., Larsen, G. (2007) Volcanism in Iceland in historical time: Volcano types, eruption styles and eruptive history. *Journal of Geodynamics 43*, 118–152.

Tuller-Ross, B., Savage, P.S., Chen, H., Wang, K. (2019) Potassium isotope fractionation during magmatic differentiation of basalt to rhyolite. *Chemical Geology* 525, 37–45.

Valley, J.W., Kitchen, N., Kohn, M.J., Niendorf, C.R., Spicuzza, M.J. (1995) UWG-2, a garnet standard for oxygen isotope ratios: strategies for high precision and accuracy with laser heating. *Geochimica et Cosmochimica Acta* 59, 5223–5231.

Webster, J.D. (1997) Chloride solubility in felsic melts and the role of chloride in magmatic degassing. *Journal of Petrology* 38, 1793–1807.

Webster, J.D. Vetere, F., Botcharnikov, R.E., Goldoff, B., McBirney, A., Doherty, A.L. (2015) Experimental and modeled chlorine solubilities in aluminosilicate melts at 1 to 7000 bars and 700 to 1250 C: Applications to magmas of Augustine Volcano, Alaska. *American Mineralogist* 100, 522–535.

White, S.M., Crisp, J.A., Spera, F.J. (2006) Long-term volumetric eruption rates and magma budgets. *Geochemistry, Geophysics, Geosystems* 7.

Willbold, M., Hegner, E., Stracke, A., Rocholl, A. (2009) Continental geochemical signatures in dacites from Iceland and implications for models of early Archaean crust formation. *Earth and Planetary Science Letters* 279, 44–52.

Yang, J., Siebert, C., Barling, J., Savage, P., Liang, Y., Halliday, A.N. (2015) Absence of molybdenum isotope fractionation during magmatic differentiation at Hekla volcano, Iceland. *Geochimica et Cosmochimica Acta* 162, 126–136.